

Lorenzo Gontrani¹, Elvira Maria Bauer², Cosimo Ricci¹, Lorenzo Casoli¹, Pietro Tagliatesta¹, Marilena Carbone¹

¹ Department of Chemical Science and Technologies, University of Rome Tor Vergata, Via della Ricerca Scientifica 1, 00133 Rome, Italy

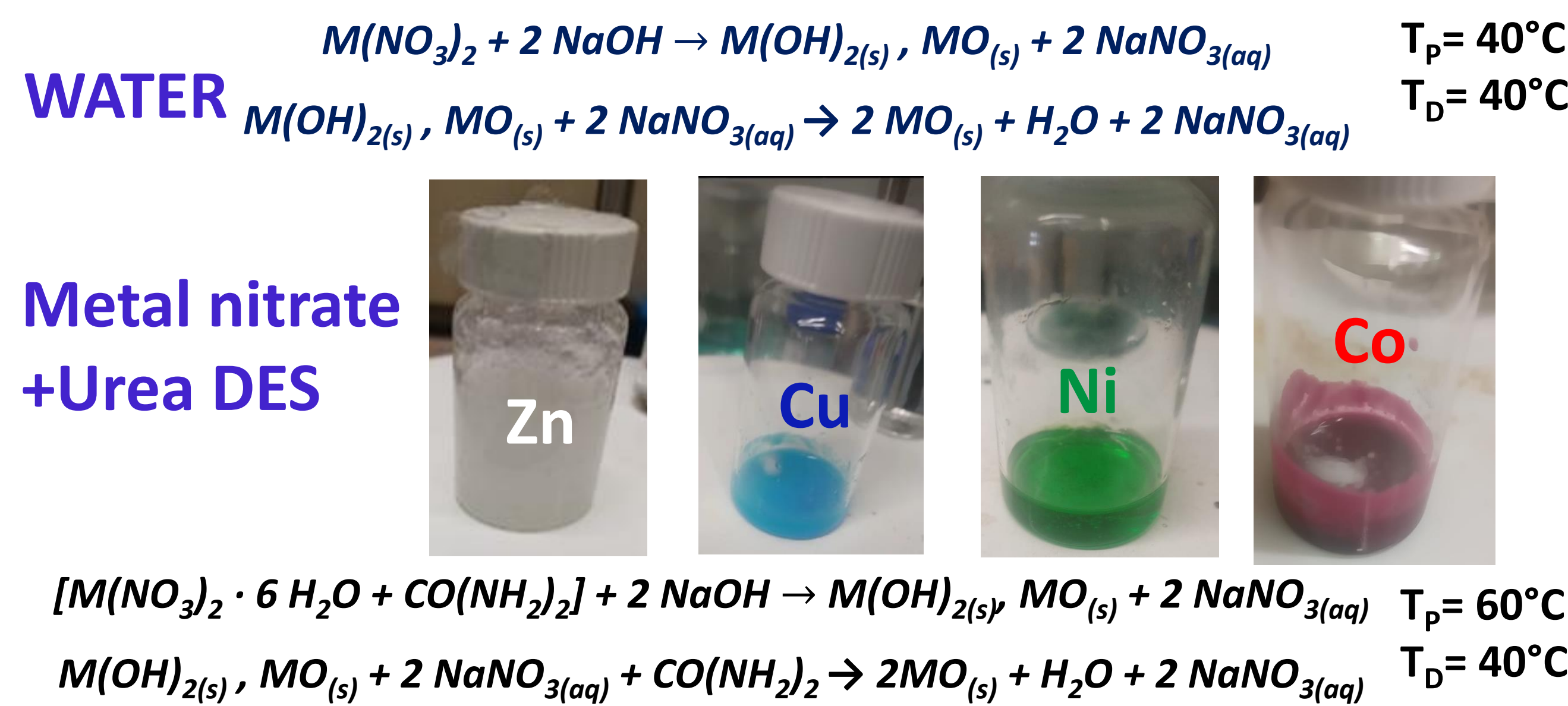
² Italian National Research Council-Institute of Structure of Matter (CNR-ISM), Via Salaria km 29.3, 00015 Monterotondo, Italy.

Introduction

The “**template effect**” is one of the most important features employed to impart **specific shapes** to nanomaterials, which very often results in tailored technological properties. It has been known for some time, for instance, that the morphology of noble metals nanoparticles is responsible for the marked variability of their optoelectronic properties. Gold NPs have various colours¹ when in colloidal solutions, or different electrical current densities when used as electrodes, if they contain. e. g. nanospheres, nanorods, nanostars or nanothorns². Here we show that **metal oxide NPs of different shapes** can be obtained following different synthesis pathways and that these manifold structures are endowed with different properties, like **variable bandgap** or **photoluminescence of different color**.

Methods

Scheme 1. (Co)precipitation reaction of metal oxide in water solution and in urea DES, example stoichiometry for a divalent metal and NaOH as base. P = Precipitation D = Drying



Water Synthesis (Zn): To a **0.1 M Zn(NO₃)₂** solution in DI water, stirred until complete dissolution, an equal volume of a **0.1 M NaOH** was added dropwise, keeping T constant in an oil bath for 24 h under agitation. The ratio between Zn(NO₃)₂ and NaOH was kept at 1:1, i.e., in excess of Zn²⁺. This implies an initial pH of 6, corresponding to the minimum ZnO water solubility (at 25 °C), to prevent the formed oxide redissolution. The slurry was digested for 2 h, centrifuged (3500 rpm/10 min), rinsed with distilled water multiple times, and then dried at T_D in oven for 72 h. Finally, a white powder was achieved³.

Synthesis in DES: The mixtures were prepared by mixing the two components (hydrated metal nitrate and urea) in **1:3.54 salt:urea** molar ratio. into sealable vials, in order to minimize humidity absorption. When the two components were put in contact, a sluggish translucent agglomerate was formed quite rapidly, which become more fluid and transparent upon gentle heating and stirring (35 – 40 °C, 600 rpm) and remained liquid at room temperature. **Equimolar** quantities of finely powdered **solid NaOH** (n moles of NaOH per mole of n-valent metal), were added to the “hot” liquid mixtures (60 °C) under stirring. A precipitate appeared after few minutes, and the system was let react for 20 minutes. The precipitate was washed with 20 mL of the desired solvent (water, ethanol) and centrifuged for 5 min at 3000 rpm after each rinse cycle. The washing procedure was stopped at pH 7 (in water), signalling that the excess of NaOH and urea had been washed out.

Results

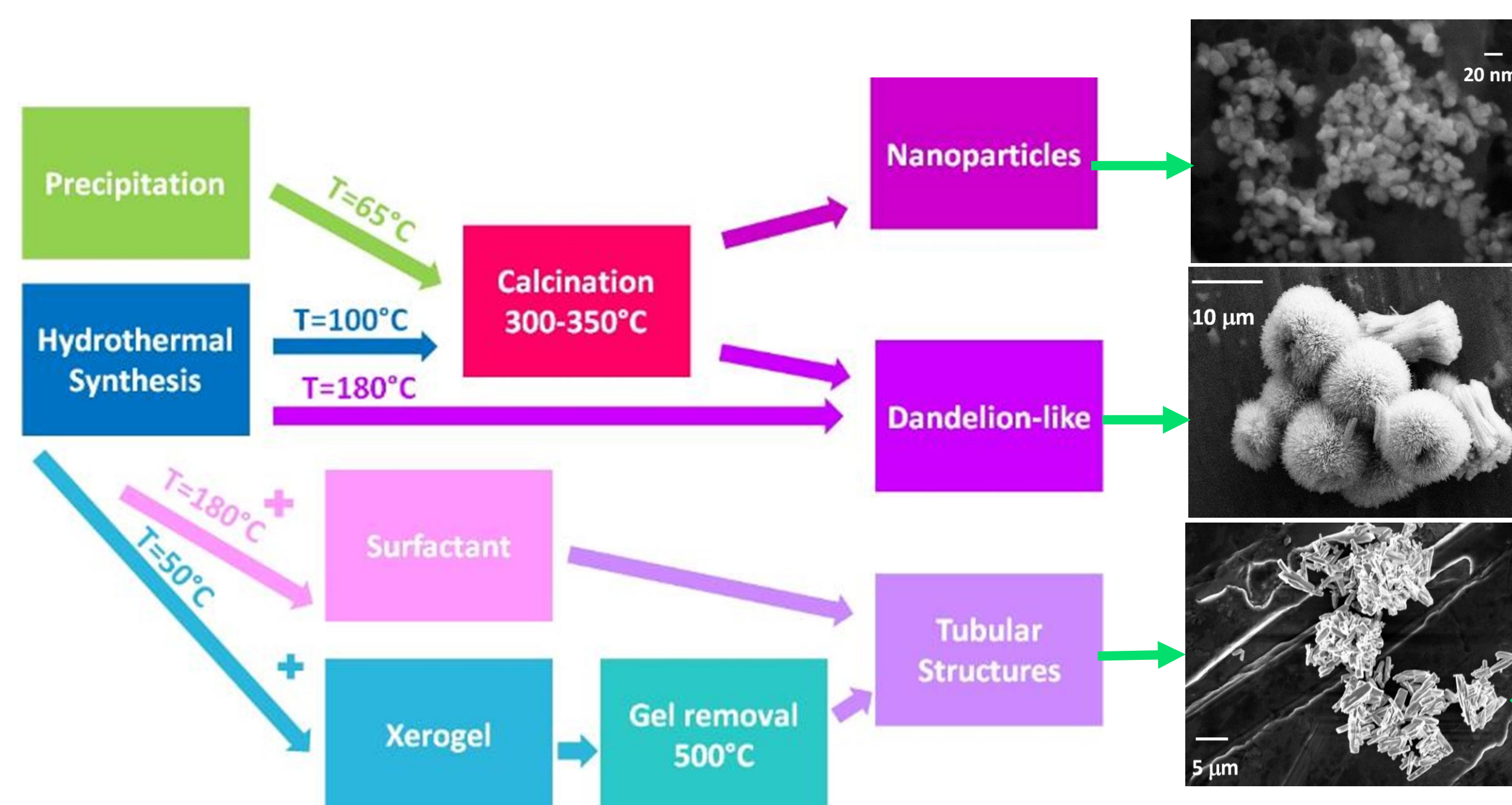


Figure 1. Systematic diagram of the conditions used for the syntheses of the CuO microaggregates and nanoparticles in aqueous environment. SEM images of some NPs synthesized

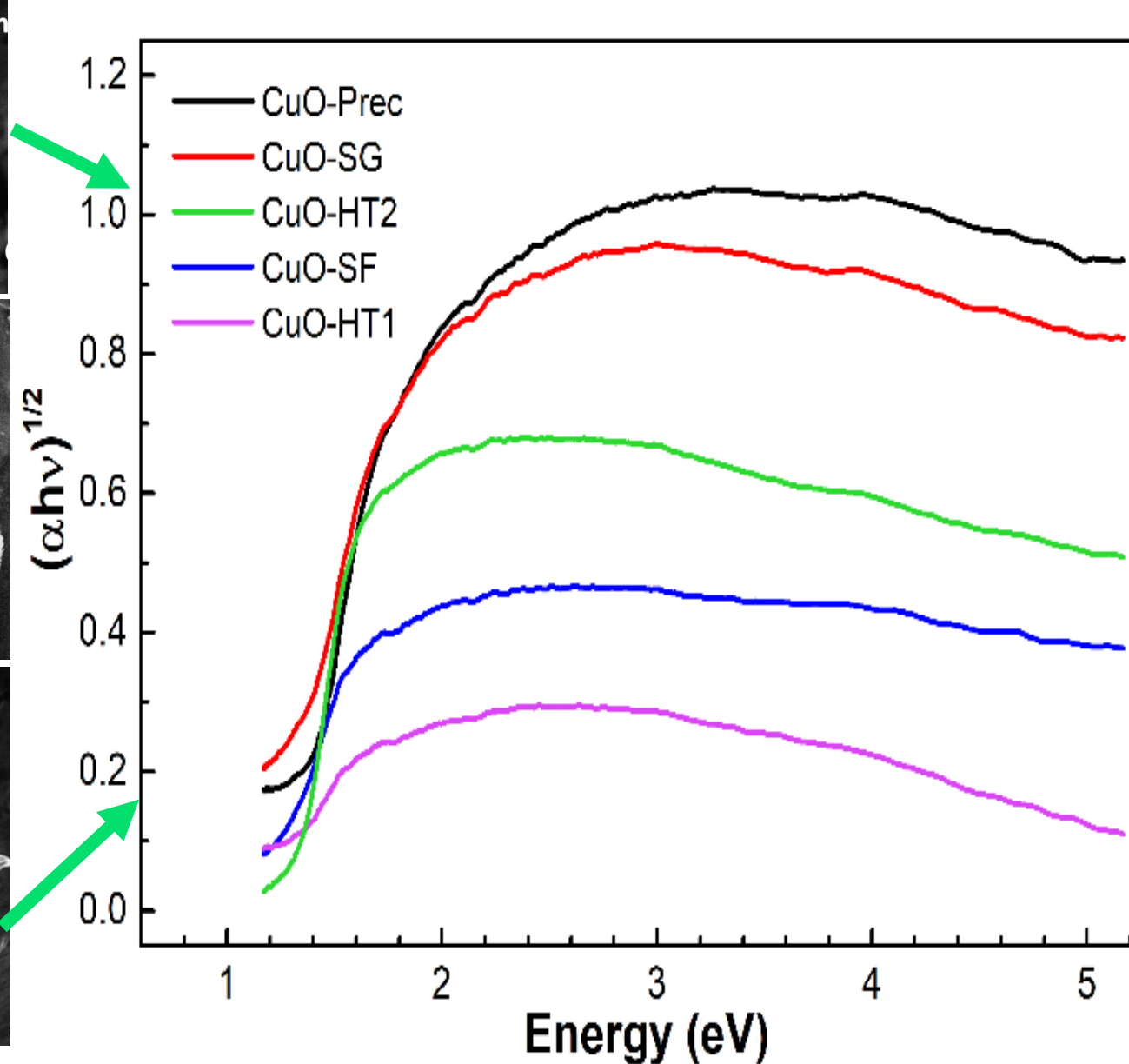


Figure 2. Tauc plot of diffuse reflectance spectra of the synthesized CuO nanoparticles.

CuO-NP samples synthesized by the hydrothermal method, are composed of spheroidal filaments in a dandelion-like arrangement, (diameter 20-100 nm, Fig. 1, middle). An alternative growth pathway when long (C16) surfactants, like CTAB, that induce a partial tubular extension of the nanostructure. Tubules of CuO-SF have, for a large part, a diameter of 100–200 nm and are re-arranged in a globular structure (Fig 1, bottom). When a precipitation procedure is followed NPs (10–20 nm size) are achieved. The UV-Vis plots were reproduced by TD-DFT using cluster models

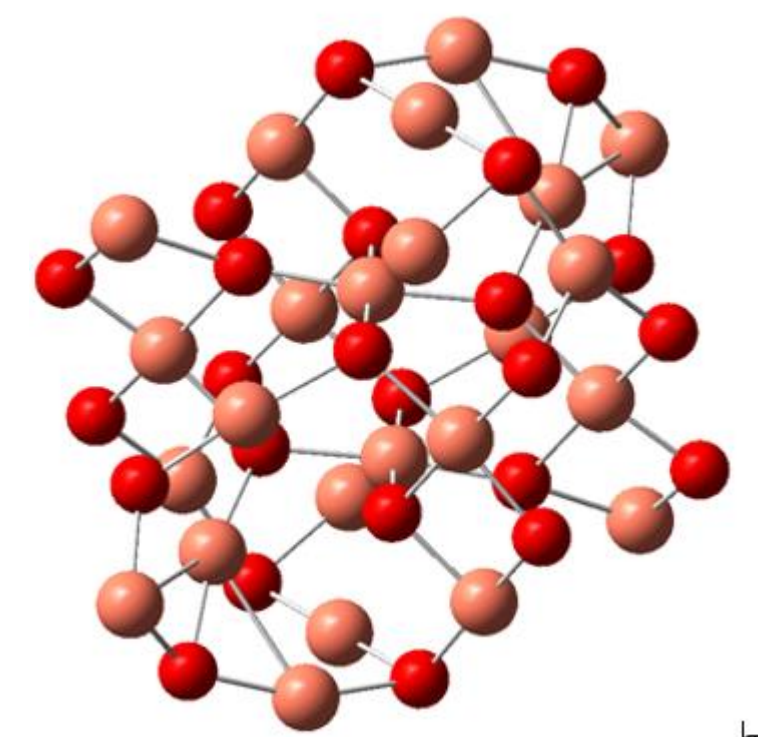


Figure 3. DFT model of CuO(24) cluster cut from tenorite crystal

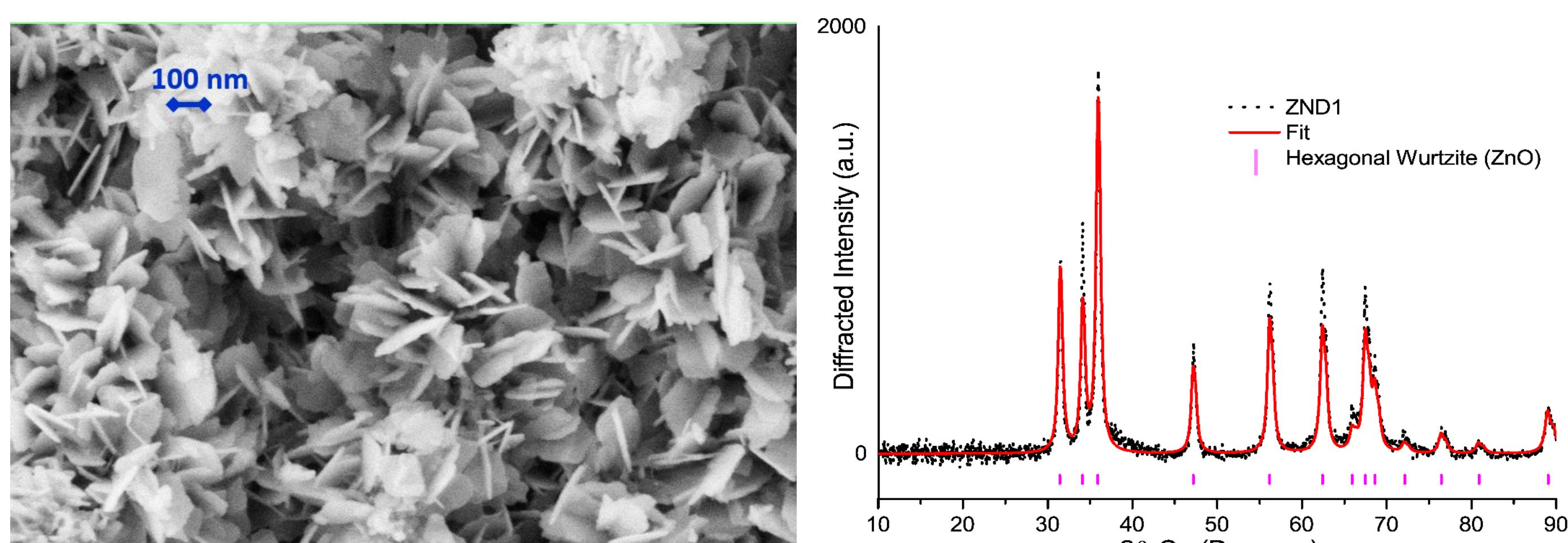


Figure 4. Sample SEM image (left), PXRD spectrum with Rietveld fit (middle) against zincite crystal (Wurtzite-type ZnO, right)

The SEM images of ZnO NPs obtained from nitrate-urea DES (Fig. 4), show that the powder is composed of layered **nanoplatelets** with longer dimension around **100 nm** and smaller dimension around **10 nm** (estimated). The NPs form flower-like assemblies extending up to 5-10 μm, composed, according to EDX microanalysis and infrared spectra, of **pure ZnO**⁵.

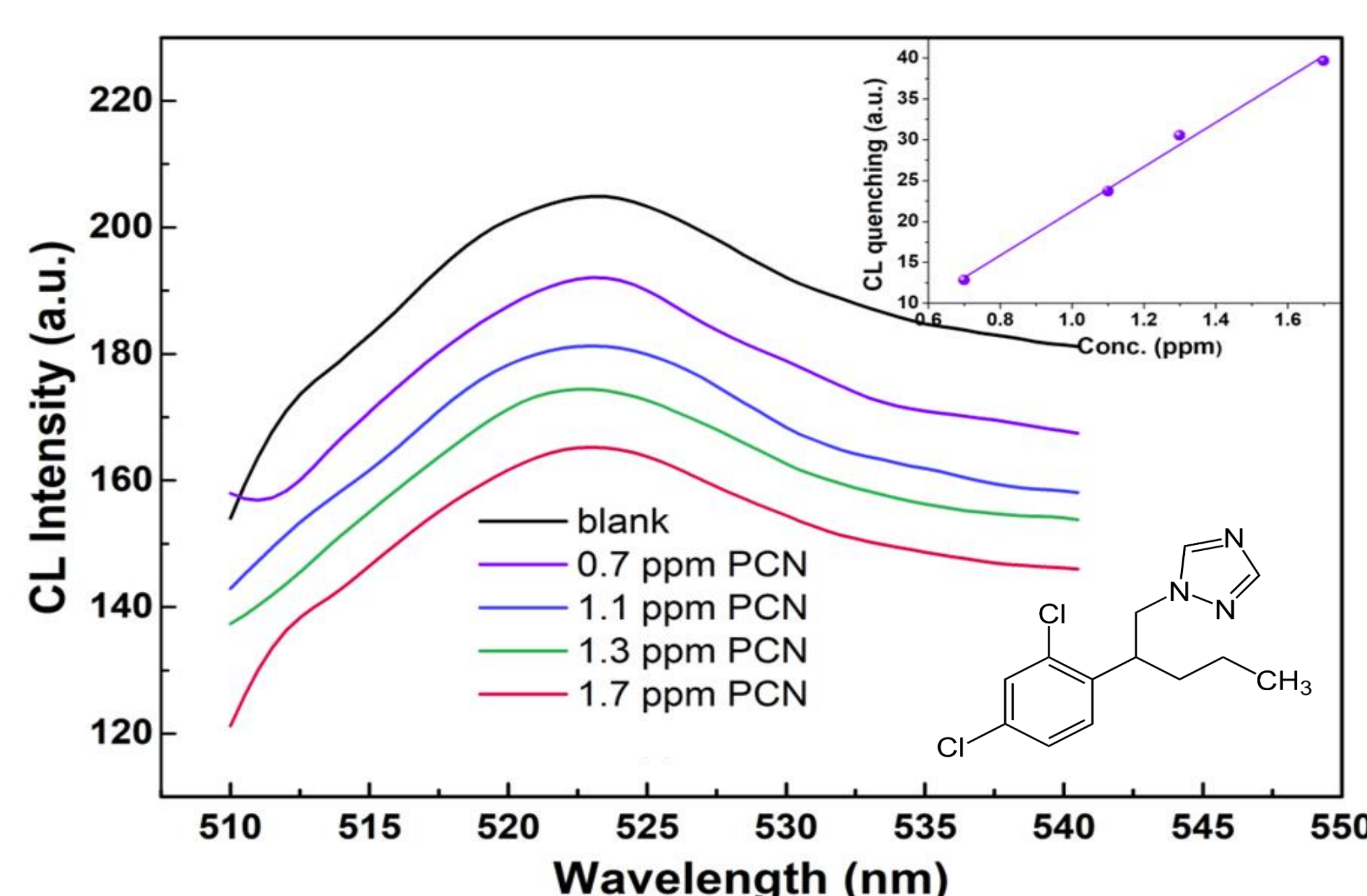


Figure 6 Chemiluminescence spectra of G-APTMS@ZnO vs penconazole (PNC, in the bottom inset) concentration. The peak intensity variation is reported in the top inset as a function of the concentration, indicating a good linear response.

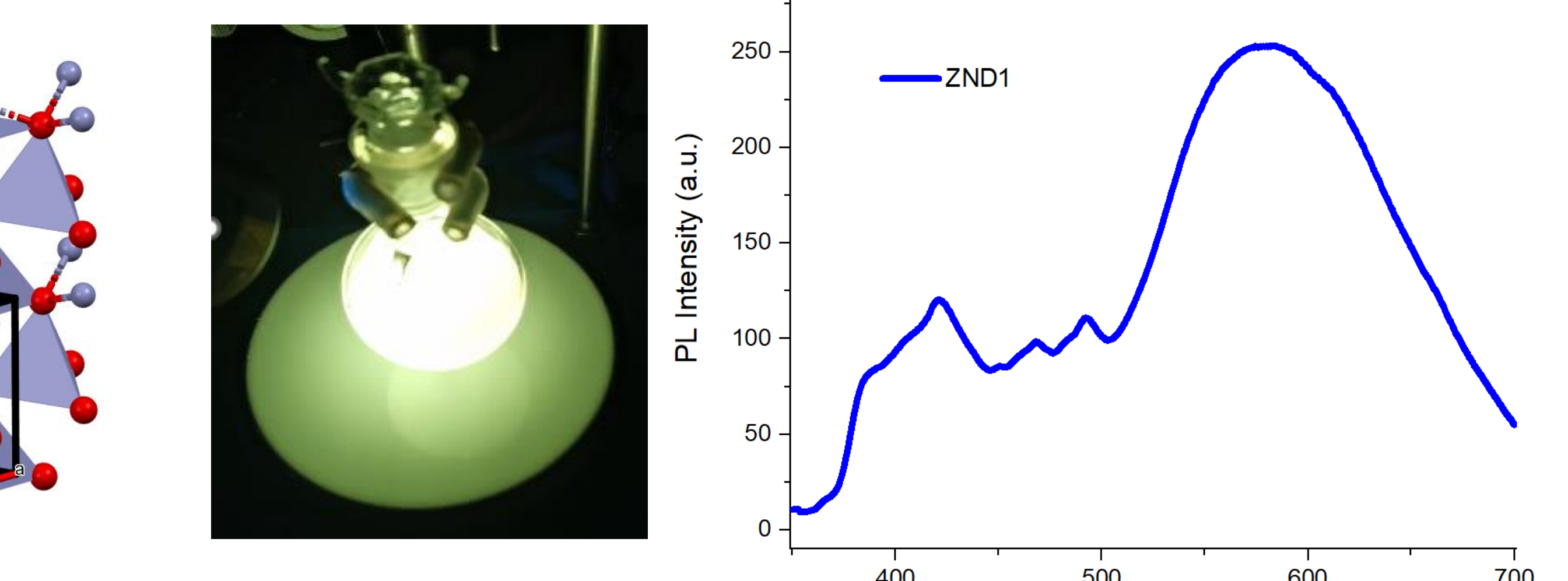
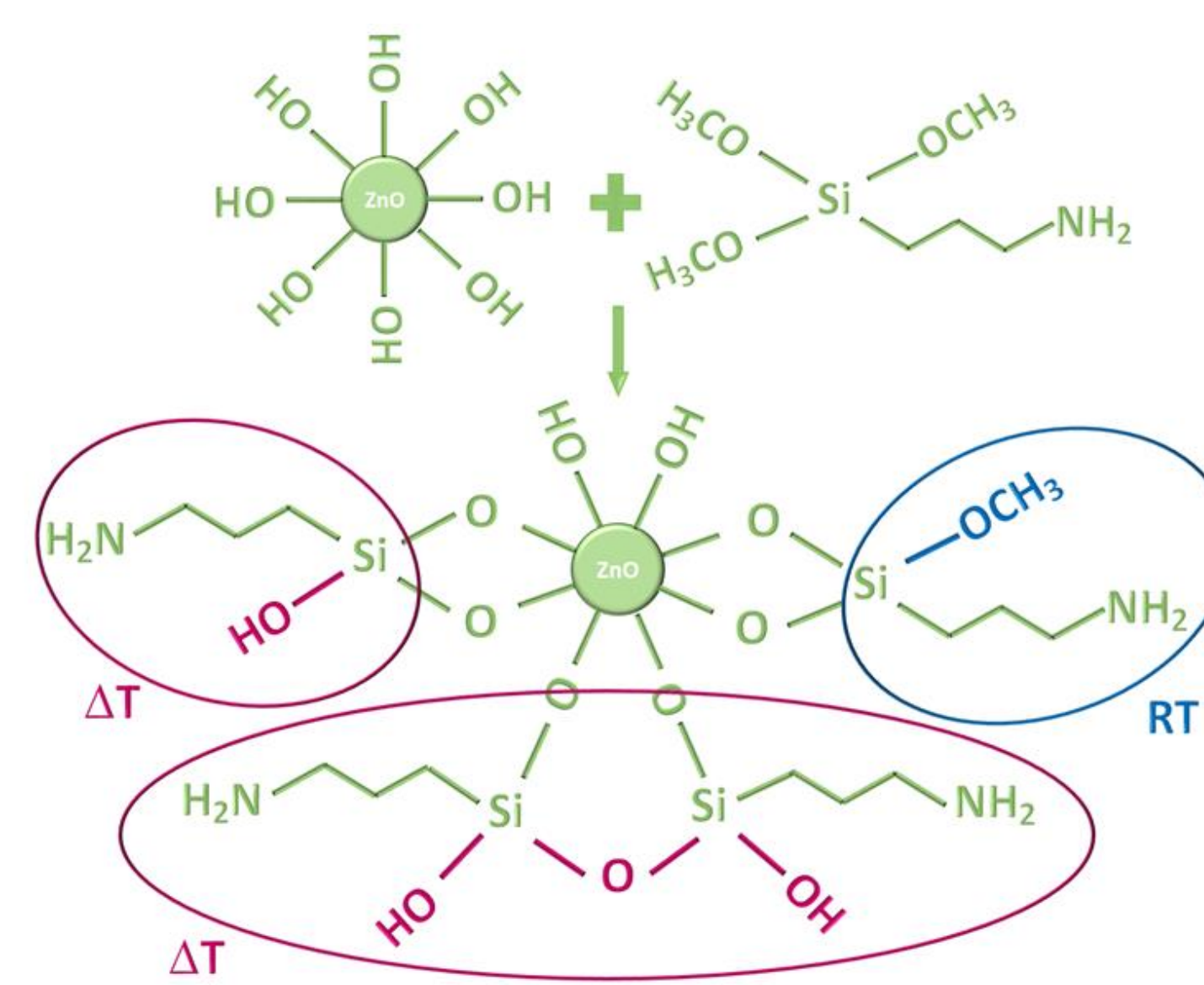


Figure 5 Strong chemiluminescence of ZnO NPs. Left: light emitted at 365 nm irradiation; right: emission spectrum in ethanol dispersion (1 mg/mL) of ZnO NPs obtained from DES under 330 nm excitation (Xe lamp)

ZnO optical properties were exploited in fluorescence-based sensing devices to detect pesticides in various matrixes. ZnO-NPs capped with APTMS as docking moiety (Scheme 2), show a remarkable linear **quenching** trend with **penconazole** concentration (between 6% and 19% of the native signal), and were able to detect it at concentration as low as **0.7 ppm**.⁶



Scheme 2. ZnO NPs capping scheme with APTMS

Acknowledgements

This research was funded by Regione Lazio within the call n. G04014-13/04/2021 “Progetti di Gruppi di Ricerca 2020”, grant number A0375-2020-36643-Sviluppo di un Dispositivo Portatile Integrato per la Valutazione Spettroscopica Multimodale non Invasiva della Qualità di Materie Prime Alimentari (B85F21001350002).

References

1. L. Freitas de Freitas, G. H. Costa Varca, J. G. Dos Santos Batista, A. Benévolo Lugão *Nanomaterials* **2018**, *8*(11), 939
2. H-G. Liao, Y-X. Jiang, Z-You Zhou, S-P. Chen, S-G. Sun. *Angew. Chem. Int. Ed.* **2008**, *47*, 9100-9103
3. D. T. Donia, E. M. Bauer, M. Missori, L. Roselli, D. Cecchetti, P. Tagliatesta, L. Gontrani, M. Carbone, *Symmetry*, **2021**, *13*, 733.
4. L. Gontrani, E. M. Bauer, A. Talone, M. Missori, P. Imperatori, P. Tagliatesta, M. Carbone, *Materials* **2023**, *16*(13), 4800
5. L. Gontrani, D. T. Donia, E. M. Bauer, P. Tagliatesta, M. Carbone, *Inorg. Chim. Acta*, **2023**, *545*, 121268
6. E. M. Bauer, G. Bogliardi, C. Ricci, D. Cecchetti, T. De Caro, S. Sennato, A. Nucara, M. Carbone, *Materials* **2022**, *15*(22), 8050